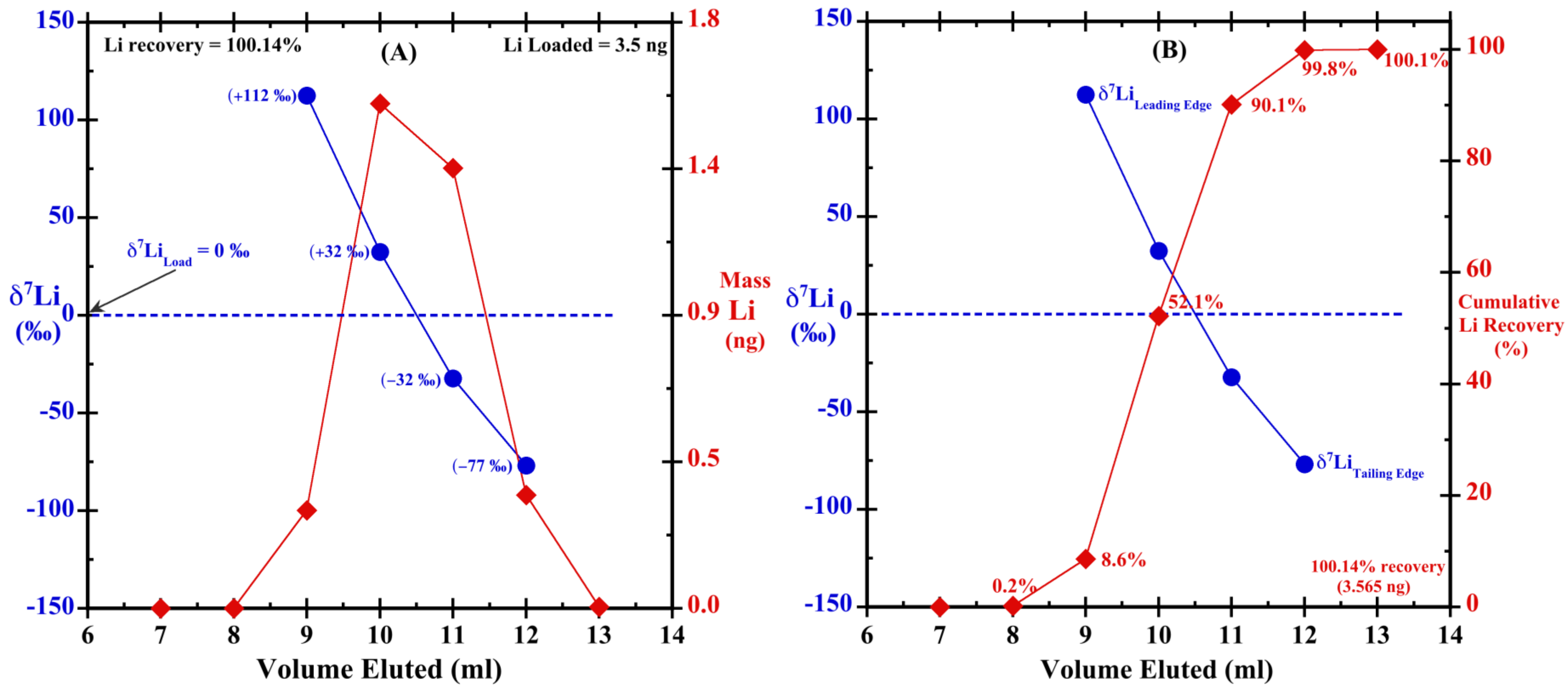

Supplementary Fig. 1 (A & B): Evolution of Li isotopic composition of during column elution. Lithium isotope ratio (δ^7Li) of column eluted fractions (solid blue circles) are plotted on the primary Y-axis in both panels A & B. In panel A, Li concentration of eluted fraction (open red diamonds) and in panel B, cumulative Li mass recovery (solid red diamonds) are plotted on the secondary Y-axis. The elution volumes (6 ml to 14 ml) are plotted on X-axis. The column was loaded with 3.5 ng of L-SVEC NIST 8545 (δ^7Li $_{\text{L-SVEC}}$ = 0‰). The elution was done volumetrically and both the concentration and isotope ratio determination of Li was done on QQQ-ICP-MS

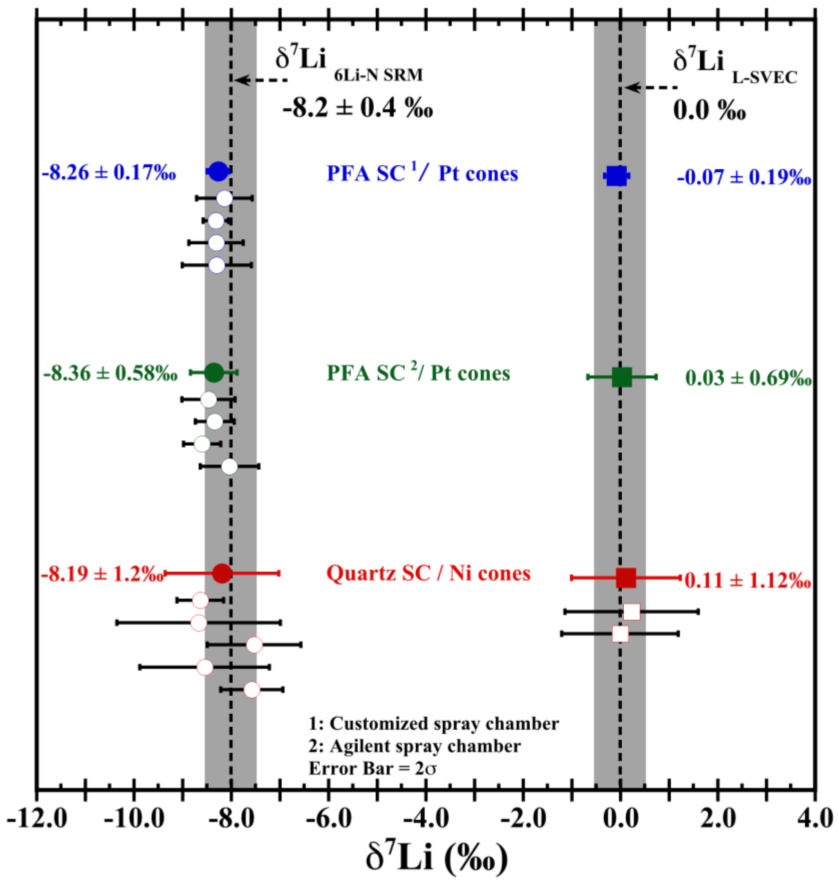

Supplementary Fig. 2. Comparison of accuracy and precision of δ^7Li determination for different mass spectrometer front end settings. The δ^7Li values are plotted on the primary X-axis. Two different standards, NIST-L-SVEC (squares) and Li-6 N SRM (circles), were analyzed following SSB protocol against concentration matched NIST L-SVEC for the comparison. The open symbols represent triplicate measurements during an instrument session. The average of individual sessions is represented by solid symbols. Error bars represent 2σ analytical uncertainty. The gray area represents ±0.5‰ window of analytical uncertainty.

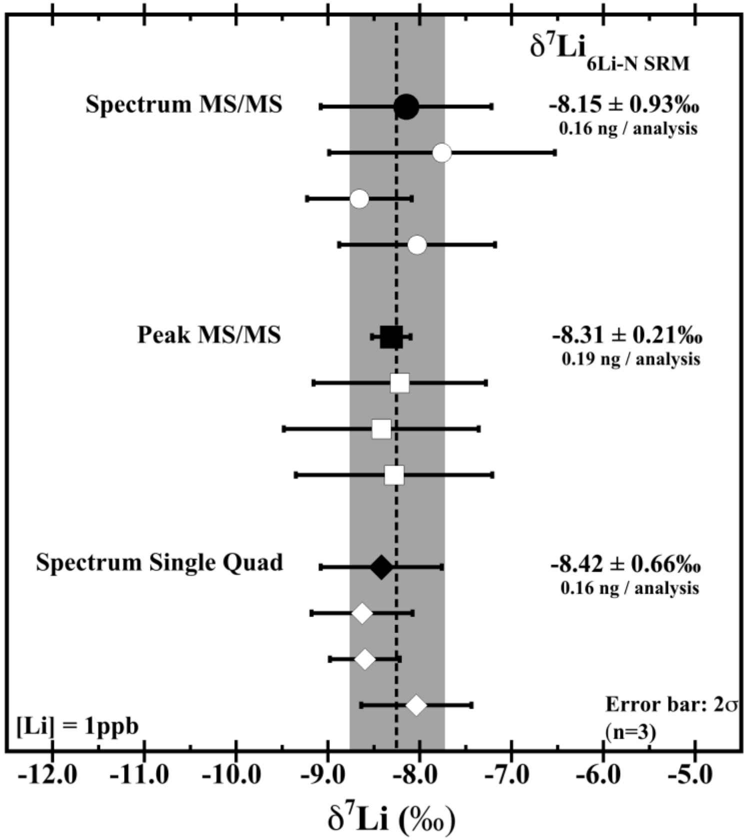

Supplementary Fig. 3. Comparison of accuracy and precision of different combination of scan modes utilized for δ^7Li determination. The δ^7Li values are plotted on primary X-axis. Open symbols represent triplicate individual analysis and the session averages are represented by solid symbols. The secondary standard 6Li N-SRM (-8.2‰) at 1 ng ml^{-1} [Li] was analyzed against concentration matched NIST L-SVEC following SSB protocol for the comparison of scan modes. Three combinations of scan modes investigated are: (i) Spectrum MS/MS mode (circles), (ii) Peak MS/MS mode (squares); and (iii) Spectrum single Quad (diamonds). The vertical dashed line represents the accepted value of the standard 6Li-N SRM (-8.2‰). Error bars represent 2σ analytical uncertainty. The gray area represents ±0.5‰ window of analytical uncertainty.

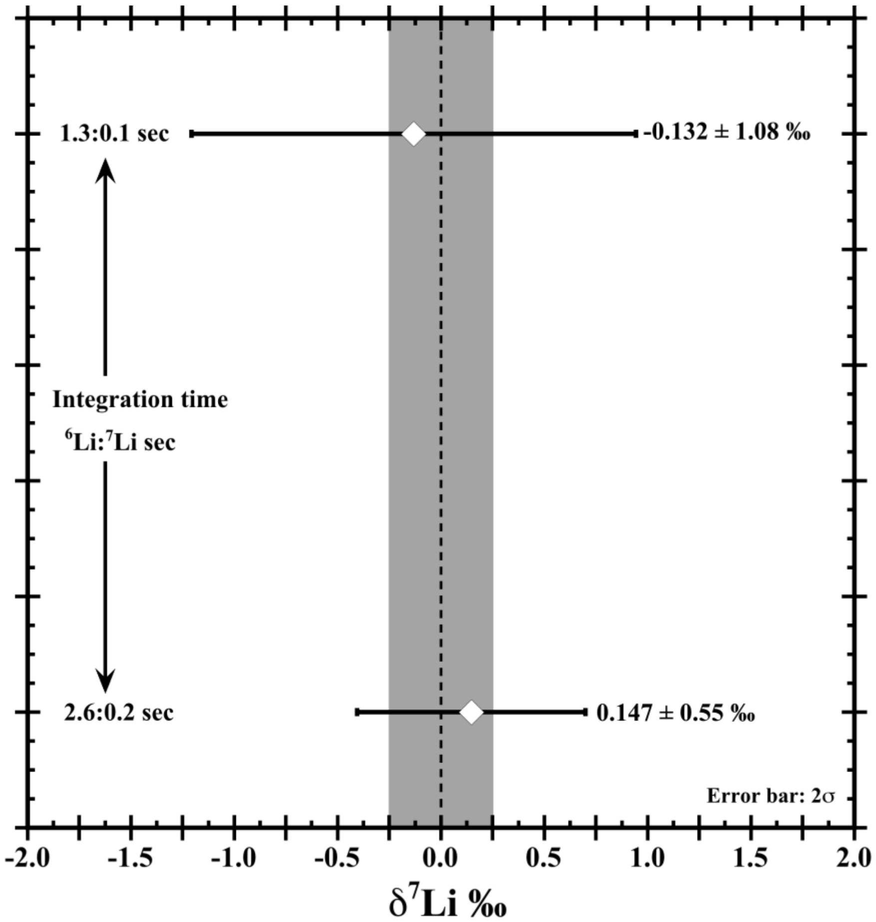

Supplementary Fig. 4. Comparison of precision and accuracy obtained from two different integration time setting for ^{6}Li and ^{7}Li. The $\delta^{7}Li_{L\text{-}SVEC}$ values are plotted on primary X-axis. Open diamonds represents δ^{7}Li values of L-SVEC measured in quintuplicate. Error bars represent 2σ analytical uncertainty. The gray area represents ±0.5‰ window of analytical uncertainty.

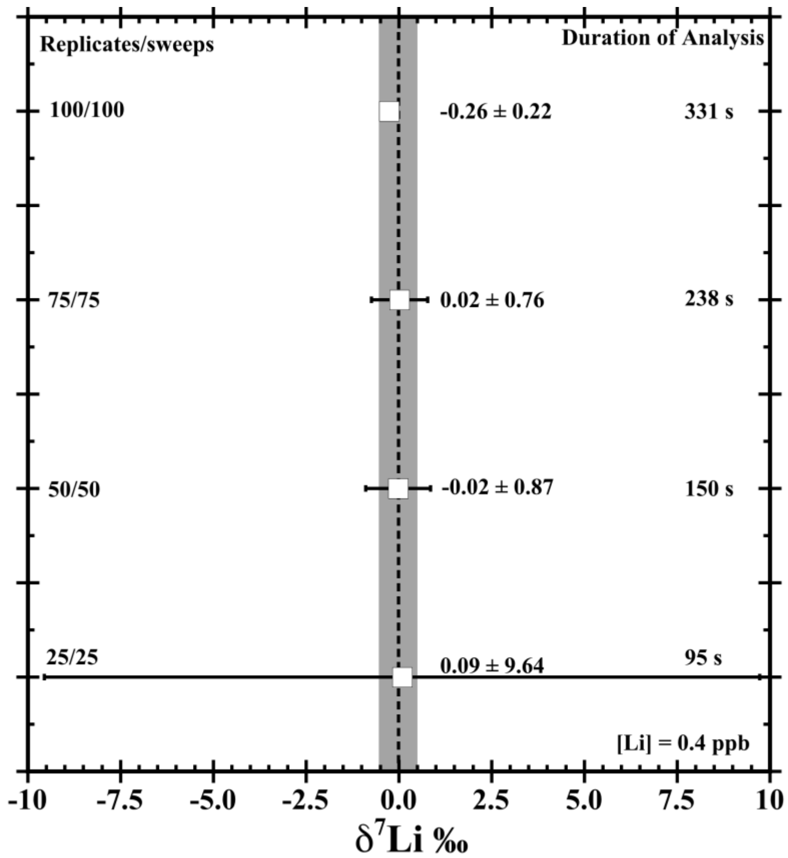

Supplementary Fig 5. Impact of choice of replicates and sweeps on the accuracy and precision of δ^7Li determination. The δ^7Li values are plotted on primary X-axis. The black open squares represent the average of quintuplicate δ^7Li values of L-SVEC based on sextuplicate ^{7}Li/^{6}Li ratio measurement. The $\delta^7Li_{L\text{-}SVEC}$ values are provided next to open squares for respective replicate-sweeps. The vertical dashed line represents $\delta^7Li_{L\text{-}SVEC}$ of 0‰. The time required per analysis is provided on the right side of the plot. Error bars represent 2σ analytical uncertainty. The gray area represents ±0.5‰ window of analytical uncertainty.

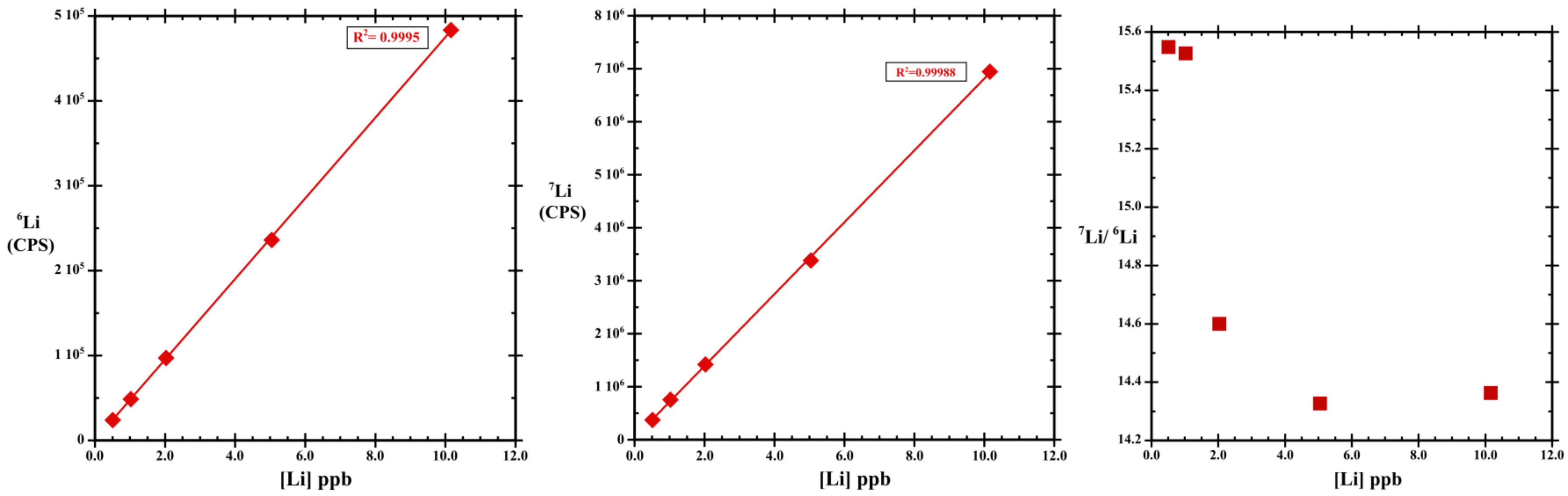

(Supplementary) Fig. 6 (A & C): Impact of ion detection mode on lithium sensitivity and mass bias ($^{7}Li/^{6}Li$). Panels A and represents ^{6}Li and ^{7}Li calibration with increasing [Li]. Panel C represents lithium mass bias with increasing [Li]. Under default instrumental settings, the switch over from pulse to analog counting happens at 1.0×10^{6} cps (observed threshold: 0.7×10^{6} cps). The ^{6}Li calibration is exclusively in pulse mode; however, the ^{7}Li calibration is in mixed mode. The switch over of ^{7}Li detection from pulse to analog mode at ion counts $>0.7 \times 10^{6}$ cps is reflected in the decrease in mass bias in Panel-C.

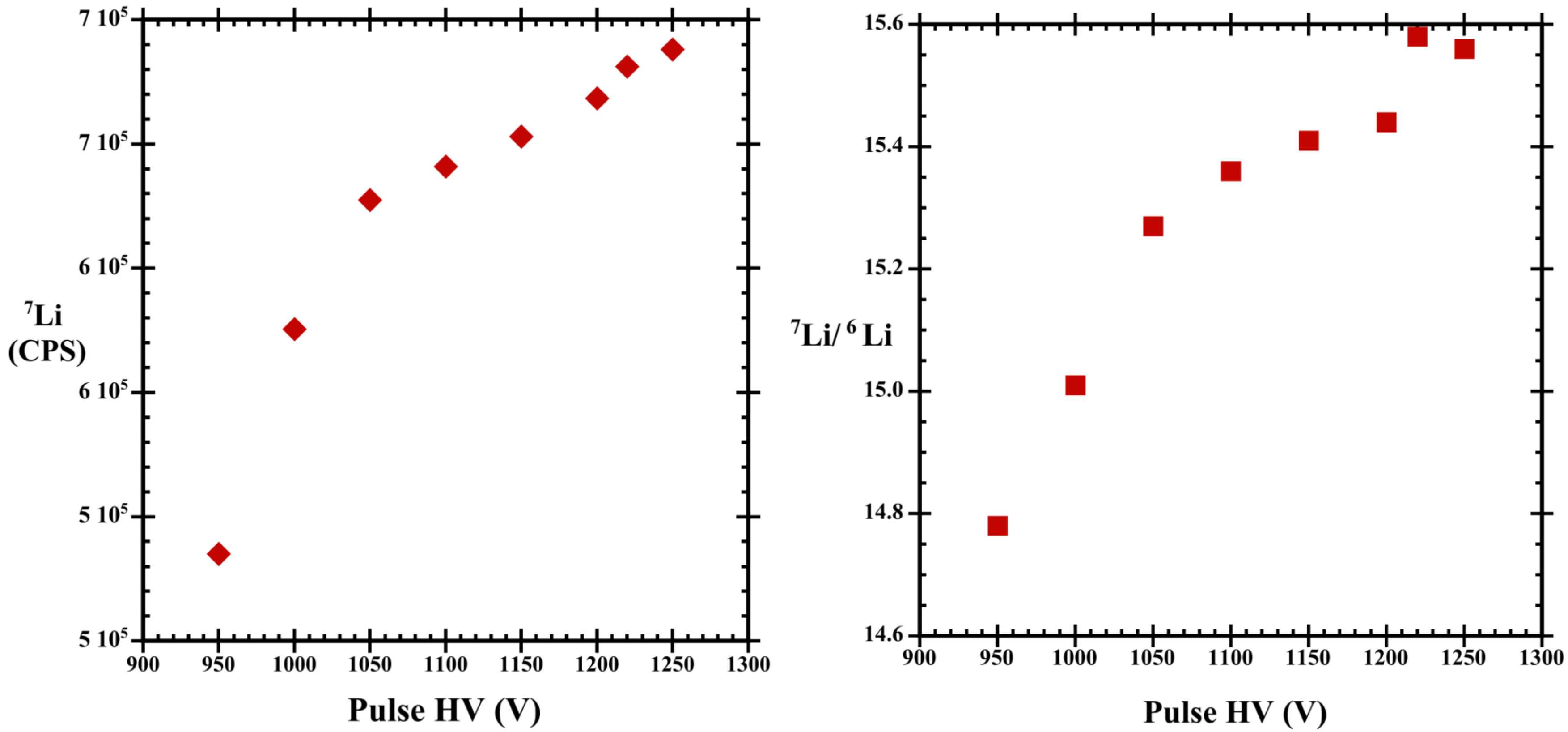

(Supplementary) Fig. 7. Response of Li sensitivity and mass bias to changes in detector Pulse HV. on within an analytical session. Pulse HV is plotted on X-axis. Lithium sensitivity (solid red diamonds) and mass bias (solid red squares) (^{7}Li/^{6}Li) are plotted on Y-axis on panels A and B respectively.

Supplementary table 1: Distribution coefficients at varying acid strengths for AG MP-50 resin

Elements	0.2N HCl	0.5N HCl	0.7N HCl	1.0N HCl	1.5N HCl	2.0N HCl
Li	22.3	9.8	7.0	5.1	4.2	3.3
Na	64	26	18.3	13.6	11.0	8.4
Mg	469	89	44.0	24.8	16.0	7.2
Ca	3700	850	604.0	214	135.5	57
Mn		161	87.9	43.6	27.5	11.3
Fe III	6600	800	568.5	89	49.5	10
Fe II		113	60.7	30	18.5	6.9
Sr	5700	1320	938.0	320	201.5	83
α_{Na-Li}	2.87	2.65	2.61	2.67		
α_{Mg-Na}				1.82	1.45	0.86

* values from Strelow et al., 1984[46]

Supplementary Table 2: Detailed Comparison of previously published column chromatography methods to the present method

Author	No. of steps	Resin type	Resin volume/ Resin height	Elution matrix	Total Elution volume (Li fraction)	Total Elution volume (Mg fraction)	Li Yield	Blank/load	Blank % wrt Li loaded
You and Chan[26]	1 step	AG 50W-X8	11.78 ml/150 mm	0.5 mol L^{-1} HCl	80 ml (42-62 ml)	-	>98%	190 pg/100 ng-Li	0.19%
James and Palmer[27]	1 step	AG 50W-X8	2.7 ml/85 mm	0.2 mol L^{-1} HCl	18 ml (24-42 ml)	-	100%	150 pg/100 ng-Li	0.15%
Hall et al.[28]	1 step	AG 50W-X8	11.78 ml/150 mm	0.5 mol L^{-1} HCl	30 ml	-	100%	57±13 pg/100 ng-Li	0.07%
Hathorne and James[29]	1 step	AG 50W-X8	4.3 ml/85 mm	0.2 mol L^{-1} HCl	45 ml (24-42 ml)	-	100%	12 pg/4 ng-Li	0.30%
Misra and Froelich[30]	1 step	AG 50W-X8	2.0 ml/250 mm	0.5 mol L^{-1} HCl	11 ml (6-11 ml)	-	100.02–99.98%	1.0 ± 0.5 pg/0.5 ng-Li	0.20%
Van Hoecke et al.[54]	1 step	AG 50W-X8	2.0, 3.0, 8.0 ml	0.5 mol L^{-1} HCl	13 ml (5-13 ml)	-	97-102%	-	-
Bohlin et al.[31]	1 step	AG MP-50	3.0 ml/250 mm	0.5 mol L^{-1} HCl	22 ml (9-22 ml)	57 ml (44-55 ml)	-	-	-
Liu et al.[41]	2 step	AG 50W-X8	1^{st} step - 17 ml; 2^{nd} step - 3.4 ml	0.7 mol L^{-1} HNO_3	85 ml (35-80 ml)	-	100%	5 pg/2.5 ng-Li	0.5%
Zhu[25]	1 step, 2 step	AG MP-50	1 ml/85 mm	0.73 mol L^{-1} HCl	17.5 ml	-	>99%	-	
This study	1 step	AG MP-50	1.5 ml/200 mm	0.5 mol L^{-1} HCl	13 ml (7-12 ml)	43 ml (37-43 ml)	101.0±1.2 %	30-100 fg/ng-Li	0.05-0.1%

Supplementary table 3: long term 6Li-N SRM data

Long term SRM#6 (6Li-N SRM) Data												
Date		d^7Li	2s	2SE	[Li]	d^7Li	2s	2SE	n	d^7Li_{avg}	2s	2SE
26/07/21	1	-8.07	1.38	0.97	1.5-2 ng/ml	-8.240	0.327	0.123	7	-8.269	0.290	0.075
27/07/21	2	-8.47	1.34	0.77	1.5-2 ng/ml							
28/07/21	3	-8.28	1.30	0.75	1.5-2 ng/ml							
28/07/21	4	-8.00	0.46	0.32	1.5-2 ng/ml							
30/07/21	5	-8.30	0.41	0.09	1.5-2 ng/ml							
10/08/21	6	-8.37	0.59	0.34	1.5-2 ng/ml							
10/08/21	7	-8.20	0.20	0.12	1.5-2 ng/ml							
19/09/21	8	-8.24	0.83	0.48	1-1.5 ng/ml	-8.266	0.203	0.102	4			
22/09/21	9	-8.40	1.45	0.84	1-1.5 ng/ml							
23/09/21	10	-8.15	0.95	0.43	1-1.5 ng/ml							
05/10/21	11	-8.27	1.10	0.55	1-1.5 ng/ml							
01/01/22	12	-8.28	0.66	0.66	0.4-1 ng/ml	-8.322	0.341	0.170	4			
02/01/22	13	-8.10	0.42	0.24	0.4-1 ng/ml							
10/02/22	14	-8.45	0.61	0.35	0.4-1 ng/ml							
11/02/22	15	-8.45	0.77	0.45	0.4-1 ng/ml							

Supplementary table 4: Reported δ^7Li seawater values

Author	d^7Li Seawater		Instrument
You and Chan[26]	32.4 ± 2.6 ‰	(2s, n=6)	TIMS
Chan and Edmond[6]	33.3 ± 1.2 ‰	(2s, n=5)	TIMS
Moriguti and Nakamura[8]	30.0 ± 0.7 ‰	(2s, n=5)	TIMS
James and Palmer[27]	32.5 ± 1.6 ‰	(2s, n=7)	TIMS
Hall et al.[28]	33.0 ± 1.2 ‰	(2s, n=7)	TIMS
Tomascak et al.[36]	31.8 ± 1.9 ‰	(2s, n=15)	MC-ICP-MS
Nishio and Nakai[52]	29.3 ± 0.9 ‰	(2s, n=3)	MC-ICP-MS
Bryant et al.[37]	31.0 ± 1.8 ‰	(2s, n=18)	MC-ICP-MS
Jeffcoate et al.[38]	31.14 ± 0.2 ‰	(2s, n=32)	MC-ICP-MS
Hathorne and James[29]	31.0 ± 0.5 ‰	(2s, n=6)	MC-ICP-MS
Misra and Froelich[30]	30.75 ± 0.45 ‰	(2s, n=10)	Q-ICP-MS
Toki et al.[53]	30.9 ± 0.3 ‰	(2s, n=7)	MC-ICP-MS
Bohlin et al.[31]	30.27 ± 0.40‰	(2s, n=30)	MC-ICP-MS
Liu et al.[41]	30.42 ± 0.97 ‰	(2s, n=3)	Q-ICP-MS
Zhu et al.[25]	31.62 ± 0.22 ‰	(2s, n=4)	MC-ICP-MS
This study	31.34 ± 0.56 ‰	(2s, n=49)	QQQ-ICP-MS